

Anytime Neural Prediction via Slicing Networks Vertically

Hankook Lee * Jinwoo Shin *

July 10, 2018

Abstract

The pioneer deep neural networks (DNNs) have emerged to be deeper or wider for improving their accuracy in various applications of artificial intelligence. However, DNNs are often too heavy to deploy in practice, and it is often required to control their architectures dynamically given computing resource budget, i.e., anytime prediction. While most existing approaches have focused on training multiple shallow sub-networks jointly, we study training thin sub-networks instead. To this end, we first build many inclusive thin sub-networks (of the same depth) under a minor modification of existing multi-branch DNNs, and found that they can significantly outperform the state-of-art dense architecture for anytime prediction. This is remarkable due to their simplicity and effectiveness, but training many thin sub-networks jointly faces a new challenge on training complexity. To address the issue, we also propose a novel DNN architecture by forcing a certain sparsity pattern on multi-branch network parameters, making them train efficiently for the purpose of anytime prediction. In our experiments on the ImageNet dataset, its sub-networks have up to 43.3% smaller sizes (FLOPs) compared to those of the state-of-art anytime model with respect to the same accuracy. Finally, we also propose an alternative task under the proposed architecture using a hierarchical taxonomy, which brings a new angle for anytime prediction.

1 Introduction

Deep neural networks (DNNs) have demonstrated state-of-the-art performance on many artificial intelligence applications such as speech recognition [12], image classification [9], video prediction [33] and medical diagnosis [3]. One of key components underlying their success is on advanced DNN architectures such as AlexNet [21], VGGNet [28], Inception [30], ResNet [13] and DenseNet [16]. Although they were originally developed for image classification, they also have provided influential impacts on designing deep and wide network architectures for other related tasks, e.g., 3D-object reconstruction [4], super-resolution [23], image compression [32] and image generation [29].

However, the heavy models are often not suitable for real-world applications due to their resource budgets, e.g., limited memory in mobile devices, low latency for autonomous driving and real-time constraints for Internet video delivery. Motivated by this, extensive research efforts recently have been made for designing light neural networks of high performance under various approaches, e.g., network pruning [11, 24] and transfer learning [27, 15]. However, they are primarily targeting a single resource budget constraint. Hence, if an application should work under various resource budgets adaptively or the computing power of clients' device is heterogeneous, then all models of various sizes should be ready separately. It is too inefficient to train and store.

*School of Electrical Engineering, Korea Advanced Institute of Science and Technology, Daejeon, Korea (hankook.lee@kaist.ac.kr, jinwoos@kaist.ac.kr)

For such applications, designing a single model which can operate under various computational resource budgets dynamically is very important. The problem is often called *anytime/adaptive prediction* [36, 10]. Most recent works on this line [31, 25, 2, 7, 19, 17] use intermediate features of DNN, possibly attached by additional classifiers to produce multiple outputs at different layers. That is, shallower and deeper sub-networks are used under smaller and larger resources (but, lower and higher accuracy), respectively, on demand. However, joint-training all such sub-networks together is not easy since shallower ones cannot capture level features, and deeper ones might be badly trained if one forces intermediate layers to produce the final outputs. To tackle the challenge, multi-scale inputs/features [25, 17] and dense connections [17] have been used, but shallow sub-networks should fundamentally suffer from lack of expressive capacity in feature representation.

Contribution. To overcome the fundamental limitation on training shallow sub-networks jointly, we aim for doing *thin* ones instead. To this end, we first observe that many recent state-of-the-art DNN architectures of residual-type have multiple branches at each block. We consider their inclusive thin sub-networks obtained by removing some branches of the full-network in a progressive manner while keeping the original depth. Then, we train all sub-networks (including the full-network) jointly under a minor modification: each sub-network has independent batch normalization layers [18]. This simple approach is promising as it is based on existing multi-branch DNNs that have achieved the state-of-art performance for the standard, non-anytime prediction task.

Our first major founding is that the performance of the full-network, named I(nclusive)-ResNeXt under the joint training is not degraded much compared to the original solely trained network without considering sub-networks. In other words, I-ResNeXt is able to make each sub-network perform their own functionality of high performance. In our experiments, I-ResNeXt, significantly outperforms the state-of-art anytime prediction model, MSDNet [17] on CIFAR datasets. In particular, its sub-networks have up to 56.0% and 48.7% smaller sizes (FLOPs) compared to those of MSDNet of the same accuracy on CIFAR-10 and CIFAR-100, respectively.

However, the above simple approach has the following drawback: training its K thin sub-networks jointly requires K independent (forward and backward) propagation passes at each iteration, making the overall training procedure K times slower. Here, we remark that joint-training all shallow networks, e.g., in MSDNet, requires only a single propagation pass at each iteration due to their interruptible property. To address the training issue, we propose a novel multi-branch architecture whose thin sub-networks can be trained jointly using a single propagation pass at each iteration. In particular, we design a sparse version of I-ResNeXt, named IS-ResNeXt by enforcing a certain sparsity pattern of network parameters: IS-ResNeXt is K times faster to train, enabling us to apply it to large-scale datasets. In our experiments, sub-networks of IS-ResNeXt have up to 43.3% smaller sizes (FLOPs) compared to those of MSDNet of the same accuracy on the ImageNet [5] dataset.

Finally, we also try an alternative task, called hierarchical anytime prediction, assuming the hierarchical taxonomy is available. In this case, a model is allowed to predict coarse-level labels in the taxonomy for maintaining the original accuracy level across all resource budgets. Namely, it is better to produce less-informative predictions rather than incorrect ones. We show that the proposed IS-ResNext also works well for the new problem, e.g., the taxonomy information allows us to improve the worst-case accuracy $31.2\% \rightarrow 47.5\%$ of sub-networks on the Caltech-UCSD Birds [34] dataset. While the improvement might be not surprising as we allow to lose the predictive information for small sub-networks, this new task provides a new angle toward a practical anytime predictor and show the robustness of our architectures under significantly more tasks to perform.

2 Preliminaries

2.1 Anytime prediction under shallow neural sub-networks

We first describe the model of anytime prediction [10] and its training loss. Let $f : \mathbf{x} \rightarrow \hat{y}$ be a model and $\tau(f)$ be its computational cost. The cost function τ can be actual CPU/GPU time or the number of multiply-addition operations (FLOPs). In this paper, we use FLOPs as the measure as it only depends on models (not devices). For given time T , let $f_{\langle T \rangle} : \mathbf{x} \rightarrow \hat{y}$ be a restriction of the model f with $\tau(f_{\langle T \rangle}) \leq T$. One can say that f is an anytime predictor if $f_{\langle T \rangle}$ can produce an output of high quality for any time budget T . There are several desirable properties for anytime predictors [36]: *monotonicity* - the quality of predictions is non-decreasing over time budgets; *optimality* - the quality at any time budget is close to the optimal quality under it; *interruptibility* - the predictor can be stopped at any time with predictions. Here, the interruptibility is useful when the time budget T is unknown when an input \mathbf{x} is ready to process. However, in many practical scenarios, one can decide T in advance, e.g., environments typically change slowly compared to $\tau(f)$ or the client’s device information is available.

Let f_1, f_2, \dots, f_K be the possible restrictions of an anytime predictor f . Then, for a given training dataset \mathcal{D} , the loss for anytime prediction can be defined as the following:

$$\mathcal{L}_{\text{anytime}}(\mathcal{D}, f) = \frac{1}{|\mathcal{D}|} \sum_{(\mathbf{x}, y) \in \mathcal{D}} \sum_{k=1}^K \mathcal{L}(y, f_k(\mathbf{x})), \quad (1)$$

where \mathcal{L} is a loss (e.g., cross entropy) between ground-truth and model-prediction.

In the case of a DNN f , it is natural to consider shallow sub-networks as the restriction models $\{f_k\}$. Let $h^{(l)}$ be the l -th layer function and $\mathbf{x}^{(l)}$ be the input of $h^{(l)}$, i.e., $\mathbf{x}^{(l+1)} = h^{(l)}(\mathbf{x}^{(l)})$. Then, one can produce an output by using an intermediate feature $x^{(l_k+1)}$, i.e., $f_k(\mathbf{x}) = g_k(\mathbf{x}^{(l_k+1)})$ where g_k be an auxiliary output function (or classifier). In this case, only the first l_k layers are required to compute, i.e., the output can be produced from a shallow sub-network. Since the sub-network is more efficient to compute, one might hope to choose it instead of the full-network for faster inference (but, potentially sacrificing accuracy) on demand. However, obtaining good shallow sub-networks and the full-network together, i.e., training them jointly sharing parameters, is fundamentally difficult because (a) an auxiliary output function connected to an intermediate layer under a shallow sub-network cannot capture both coarse-level and high-level features and (b) forcing the intermediate features to produce outputs might degrade performance of the full-network. This phenomenon hurts the desired optimality of anytime prediction: the overall performance of shallow sub-networks are degraded compared to the case of training them separately/independently without sharing their parameters. We provide experimental supports on this in Section 4.1.

2.2 Multi-branch neural architectures

For developing better anytime prediction models, we focus on multi-branch DNN models which include many existing state-of-the-art architectures, e.g., Inception [30], FractalNet [22], ResNet [13] and DenseNet [16]. They commonly apply the following module/block, repeatedly for building deep models. Let \mathcal{F}_i be the i -th branch that can be any function, e.g., neural networks or polynomials, and \mathcal{A} is a function aggregating them, e.g., addition or concatenation. For an input \mathbf{x} , the branches of a block process it independently, and then the block aggregates them to produce an output \mathbf{y} as

$$\mathbf{y} = \mathcal{A}(\mathcal{F}_0(\mathbf{x}), \mathcal{F}_1(\mathbf{x}), \dots, \mathcal{F}_C(\mathbf{x})).$$

By using the output \mathbf{y} as an input of the next block iteratively, deeper networks can be constructed.

One can immediately observe that ResNet is a two-branch architecture having the identity branch $\mathcal{F}_0(\mathbf{x}) = \mathbf{x}$ and the additive aggregation, i.e., $\mathbf{y} = \mathbf{x} + \mathcal{F}(\mathbf{x})$. The ResNeXt [35] architecture is an extension of ResNet: the former has more explicit branches and often outperforms the latter, e.g., ResNeXt achieved the 2nd place on the Large-Scale Visual Recognition Challenges (ILSVRC) 2016 classification task and state-of-the-art accuracy on CIFAR datasets with additional regularization technique [8]. ResNeXt uses a single identity branch as like ResNet and additional branches $\{\mathcal{F}_i\}_{i=1,2,\dots,C}$ with the same neural topology consisting of three convolutional layers with batch normalization (BN) and ReLU activations, i.e., $\mathbf{y} = \mathbf{x} + \sum_{i=1}^C \mathcal{F}_i(\mathbf{x})$. The first and third convolution layers in each branch use 1×1 kernels and the second one uses 3×3 kernels. The first one embeds input features of width W to small-sized bottleneck features of width B , and the third one embeds reversely. Namely, the width of both input and output of the second convolutional layer is B . See Figure 1a illustrating a block of ResNeXt architecture with $C = 9$. We often say C as the number of branches or cardinality. Note that each branch \mathcal{F}_i can be parameterized by convolutional weights \mathbf{w}_i and BN parameters \mathbf{u}_i , thus one can write the block as

$$\mathbf{y} = \mathbf{x} + \mathcal{F}(\mathbf{x}; \mathbf{w}_1, \mathbf{u}_1) + \dots + \mathcal{F}(\mathbf{x}; \mathbf{w}_C, \mathbf{u}_C).$$

In this paper, we primarily focus on ResNeXt for demonstrating our approaches, but in principle, they are applicable for generic multi-branch, even non-convolutional architectures. Moreover, it is often possible to understand many neural networks as multi-branch ones even if they do not enforce them explicitly. For example, 2-layer neural network $\mathbf{y} = V\sigma(U\mathbf{x})$ with an activation function σ can be understood as a multi-branch architecture by letting $\mathcal{F}_i(x) = V_{:,i}\sigma(U_{i,:}\mathbf{x})$, i.e., the number of branches is that of columns in the weight matrix V . This implies that ResNet with basic-type residual blocks and DenseNet with bottleneck-type blocks are also multi-branch architectures since their blocks consist of two convolutional layers.

3 Anytime prediction with thin neural sub-networks

As described in Section 2.1, training shallow sub-networks jointly is difficult and thus the overall performance of the sub-networks is degraded. In this section we study another direction maintaining the same depth of sub-networks, i.e., build thin sub-networks of ResNeXt or its variants. We also introduce a new anytime prediction task using a hierarchical taxonomy.

3.1 Inclusive ResNeXt

To build thin sub-networks from ResNeXt, we just remove the same number of branches for each block. It means that each block is expressed by $\mathbf{y} = \mathbf{x} + \mathcal{F}_1(\mathbf{x}) + \dots + \mathcal{F}_{C'}(\mathbf{x})$ where $C' \leq C$ is the number of remaining branches. As the cardinality decreases, the width of bottleneck in residual blocks also decreases, i.e., smaller C' implies thinner sub-networks. For simplicity, we use $C_k = kC/K$ as cardinality of the k -th sub-network where K be the number of sub-networks of interest. Note that the maximum number of sub-networks is $K = C$. Since the $(k+1)$ -th sub-network includes the k -th one, we refer this as Inclusive ResNeXt (I-ResNeXt) that is illustrated in Figure 1. To produce final outputs for classification, we use an independent, auxiliary classifier g_k for each sub-network. We choose a shallow classifier consisting of a batch normalization, a ReLU, a global average pooling, and a fully connected layers sequentially, like ResNet-based architectures. Hence, the total number of the auxiliary parameters is quite negligible compared

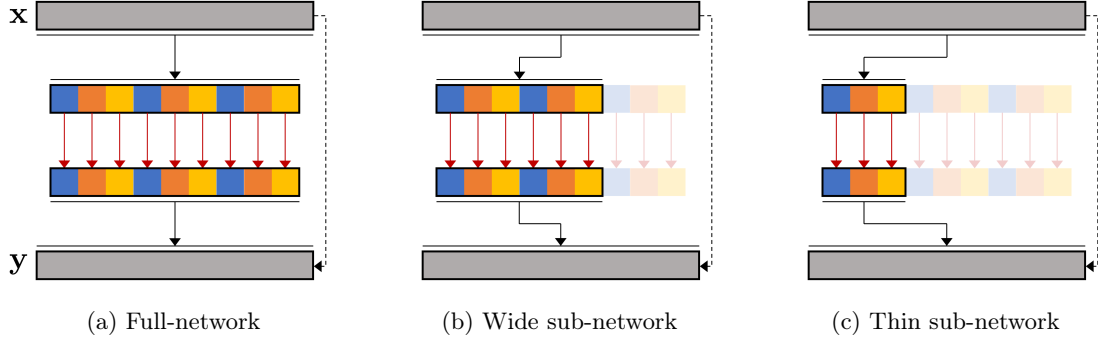


Figure 1: I-ResNeXt. The black and red solid lines are convolutions of 1×1 and 3×3 kernels, respectively. The dashed lines are identity functions. Each sub-network is built by removing branches from ResNeXt architecture. Note that sub-networks are also ResNeXt and the i -th layer’s inference result of a sub-network cannot be re-used for a different sub-network. This figure shows (a) the full-network and (b), (c) sub-networks of I-ResNeXt of $C = 9$, $K = 3$.

to that of the original ones. Then, we can express a sub-network f_k in (1) as follows:

$$f_k(\mathbf{x}) = g_k(\mathbf{x}_k^{(L+1)}), \quad \mathbf{x}_k^{(l+1)} = \mathbf{x}_k^{(l)} + \mathcal{F}(\mathbf{x}_k^{(l)}; \mathbf{w}_1^{(l)}, \mathbf{u}_1^{(l)}) + \cdots + \mathcal{F}(\mathbf{x}_k^{(l)}; \mathbf{w}_{C_k}^{(l)}, \mathbf{u}_{C_k}^{(l)}), \quad \mathbf{x}_k^{(1)} = \mathbf{x}$$

where L is the number of blocks. All sub-networks can be trained jointly by optimizing (1).

Independent batch normalization (BN) layers. During training neural networks, the input distribution at some layer changes as the previous layers are updated. This makes training parameters be more difficult. The batch normalization [18] layer alleviates this phenomenon by normalizing the input distribution as zero-mean and unit-variance. However, in our case, the number of branches is also changed while optimizing the anytime loss (1). Thus, the distribution of $\mathbf{x}_k^{(l)}$ of the k -th sub-network can be also changed depending on k . Therefore, normalizing the input distribution by universal (or shared) BN parameters \mathbf{u}_i regardless of k may not work. To handle this issue, we use independent BN parameters $\mathbf{u}_{i,k}$ for each sub-network, i.e.,

$$\mathbf{x}_k^{(l+1)} = \mathbf{x}_k^{(l)} + \mathcal{F}(\mathbf{x}_k^{(l)}; \mathbf{w}_1^{(l)}, \mathbf{u}_{1,k}^{(l)}) + \cdots + \mathcal{F}(\mathbf{x}_k^{(l)}; \mathbf{w}_{C_k}^{(l)}, \mathbf{u}_{C_k,k}^{(l)}).$$

We emphasize that the number of newly introduced parameters that are not shared among sub-networks is quite negligible compared to other shared parameters, where they are highly effective for obtaining high-performance sub-networks under the anytime loss (1). We provide experimental supports of this effect in Section 4.1.

3.2 Inclusive Sparse ResNeXt

The main issue of I-ResNext is the increased number of propagations in its training. Since the intermediate features are different among sub-networks, K propagation steps are required for training K sub-networks of I-ResNeXt at each iteration, i.e., the overall training time is K times slower than training a single ResNeXt. Due to the same reason, I-ResNext does not have the interruptibility of anytime prediction. To resolve the issue, we propose a new architecture, called Inclusive Sparse ResNeXt (IS-ResNeXt), by enforcing a certain sparsity on I-ResNeXt.

First, we split the input feature \mathbf{x} and the output feature \mathbf{y} of a block in channel-wise into K sub-features $\mathbf{x} = [\mathbf{x}_1; \dots; \mathbf{x}_K]$, $\mathbf{y} = [\mathbf{y}_1; \dots; \mathbf{y}_K]$. Our goal is to make the k -th output sub-feature \mathbf{y}_k be computable using only $\mathbf{x}_1, \dots, \mathbf{x}_k$, irrespectively of whether $\mathbf{x}_{k+1}, \dots, \mathbf{x}_K$ is removed or

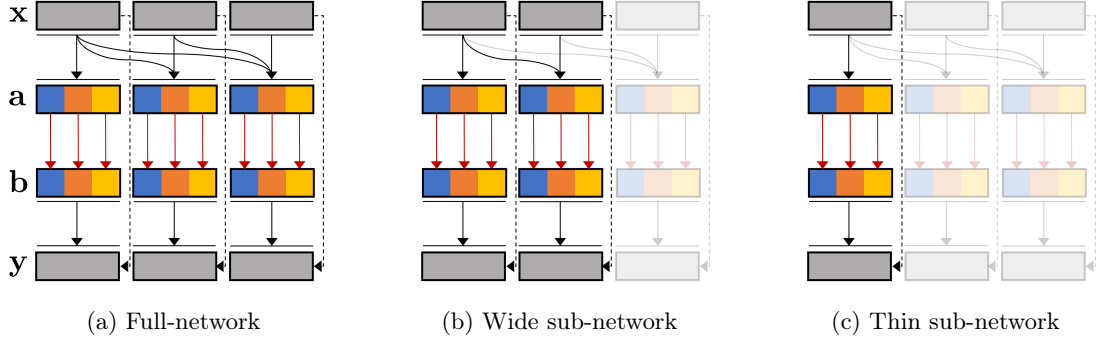


Figure 2: IS-ResNeXt. Each sub-network can be built by removing branches and reducing width of features from IS-ResNeXt architecture as described in Section 3.2. Similarly to I-ResNeXt, each sub-network is also IS-ResNeXt. Note that the k -th output sub-feature only depends on $1, \dots, k$ -th input sub-features. This property helps joint-training with thin sub-networks be efficient. This figure shows (a) the full-network and (b), (c) sub-networks of IS-ResNeXt of $C = 9$, $K = 3$.

not. Then, by using $[\mathbf{y}_1; \dots; \mathbf{y}_k]$ as the output feature of the k -th sub-network, one can obtain output features of all sub-networks by only a single forward propagation.

To describe the details, let $\mathbf{a}_1, \dots, \mathbf{a}_C$ and $\mathbf{b}_1, \dots, \mathbf{b}_C$ be the first and second intermediate features of a block in I-ResNeXt. Remark again that \mathbf{a}_i and \mathbf{b}_i have width B , and they are the input and output of 3×3 i -th convolution in the second layer, respectively. In the case of I-ResNeXt, one can observe that \mathbf{a}_i is a function of $\mathbf{x}_1, \dots, \mathbf{x}_K$ and \mathbf{y}_k is a function of $\mathbf{b}_1, \dots, \mathbf{b}_C$, i.e., $\{\mathbf{a}_i\}$ and $\{\mathbf{b}_i\}$ are densely connected to $\{\mathbf{x}_k\}$ and $\{\mathbf{y}_k\}$, respectively.

As illustrated in Figure 2, IS-ResNeXt enforces that \mathbf{a}_i be a function of $\mathbf{x}_1, \dots, \mathbf{x}_{\lceil iK/C \rceil}$ and \mathbf{y}_k be a function of $\mathbf{b}_{(k-1)C/K+1}, \dots, \mathbf{b}_{kC/K}$, i.e.,

$$\begin{aligned} \mathbf{a}_i &= \text{conv}_{1 \times 1}(\text{ReLU}(\text{BN}([\mathbf{x}_1; \dots; \mathbf{x}_{\lceil iK/C \rceil}]))), \\ \mathbf{b}_i &= \text{conv}_{3 \times 3}(\text{ReLU}(\text{BN}(\mathbf{a}_i))), \\ \mathbf{y}_k &= \text{conv}_{1 \times 1}(\text{ReLU}(\text{BN}([\mathbf{b}_{(k-1)C/K+1}; \dots; \mathbf{b}_{kC/K}]))) + \mathbf{x}_k. \end{aligned}$$

Namely, $\{\mathbf{a}_i\}$ and $\{\mathbf{b}_i\}$ are sparsely connected to $\{\mathbf{x}_k\}$ and $\{\mathbf{y}_k\}$, respectively. This sparsity provides the interruptible property, i.e., one can compute \mathbf{y}_k sequentially. Similarly to I-ResNeXt, we have the following restricted model f_k :

$$f_k(\mathbf{x}) = g_k([\mathbf{x}_1^{(L+1)}; \dots; \mathbf{x}_k^{(L+1)}]), \quad \mathbf{x}^{(l+1)} = \mathbf{x}^{(l)} + \mathcal{F}(\mathbf{x}^{(l)}; \mathbf{w}^{(l)}, \mathbf{u}^{(l)}), \quad \mathbf{x}^{(1)} = \mathbf{x}$$

where \mathbf{w} and \mathbf{u} are parameters for convolutional and BN layers, respectively. The convolutions in the third layer can be implemented by one grouped convolution like the second layer. We note that BN layers must be shared in IS-ResNeXt (in contrast to I-ResNeXt) since its sub-features are shared (or reused) among different sub-networks. We emphasize again that one can obtain all outputs of all sub-networks of IS-ResNeXt by only a single forward propagation, and also compute the gradient of (1) by only a single backward propagation.

3.3 Hierarchical anytime prediction

Under the anytime prediction task, a smaller sub-network inevitably provides a lower accuracy that might not match usable accuracy in practical applications. To address the issue alternatively,

we reformulate the anytime prediction task using a hierarchical taxonomy, where the taxonomy can be extracted from the natural language information, e.g., WordNet [26]. This approach is also motivated by a strong empirical correlation between hierarchical semantic relationships and the visual appearance of objects [6]. In the proposed hierarchical anytime prediction task, a model can predict coarse labels when small budgets are allowed, otherwise predict the original fine labels. Formally, for an input \mathbf{x} , let $\{y_d\}_{d=1,\dots,D}$ be its labels from fine to coarse, e.g., {Afghan hound, hound, hunting dog, dog} or {albatross, pelagic bird, seabird, aquatic bird, bird}. To classify these labels, we add auxiliary classifiers to all sub-networks of IS-ResNeXt (or I-ResNeXt), i.e.,

$$f_{k,d}(\mathbf{x}) = g_{k,d}([\mathbf{x}_1^{(L+1)}; \dots; \mathbf{x}_k^{(L+1)}]),$$

where $g_{k,d}$ is a classifier attached to the k -th sub-network for predicting y_d . For a given dataset \mathcal{D} , one can define the following loss to train all sub-network jointly of multi-classifiers:

$$\mathcal{L}_{\text{h-anytime}}(\mathcal{D}, f) = \frac{1}{|\mathcal{D}|} \sum_{(\mathbf{x}, \{y_d\}) \in \mathcal{D}} \sum_{k=1}^K \sum_{d=1}^D \mathcal{L}(y_d, f_{k,d}(\mathbf{x})), \quad (2)$$

which generalizes the original anytime loss (1). Once a model is trained by the above loss, one can choose appropriate coarse and fine labels targeted by small and large sub-networks so that all of them can match a certain level of accuracy, e.g., that of the solely trained one (see Section 4.3).

4 Experimental results

We evaluate our architectures for anytime prediction on CIFAR-10/100 [20], ImageNet [5] and Caltech-UCSD Birds (CUB) [34] datasets. In this section, we denote the width of features as W , the number of sub-networks as K , the number of blocks as L . We use different hyperparameters for W, K, L depending on datasets and tasks. The details of training setups and architectures are described in the supplementary material. In Section 4.1, we verify that using independent batch normalization layers improve the overall performance and utilizing thin sub-networks are more effective than shallow ones. Then, we compare ours with existing anytime prediction models in Section 4.2. Finally, we apply our architecture to a new task, named hierarchical anytime prediction, in Section 4.3.

4.1 Ablation study

Independent batch normalization layers. We first evaluate the effect of using independent BN layers when all $K = 8$ thin sub-networks of 29-layer I-ResNeXt are jointly trained under the CIFAR-10 dataset. As shown in Figure 3a, the sub-networks have poor performance when using shared BN layers. In particular, the thinnest sub-network has more than 70% classification error. On the other hand, using independent BN layers makes all sub-networks be trained stably, and reduces the classification errors of all sub-networks. As a result, the thinnest and full network achieve 12.9% and 7.2% errors which are 81.7% and 19.6% smaller than those using shared BN layers, respectively.

After joint-training with independent BN layers, we observe that the branches of I-ResNeXt are learned in a progressive manner. For example, as shown in Figure 3b, the ℓ_1 -norm of weight of the third convolutional layer of a branch in the fifth block of the 29-layer I-ResNeXt decreases as the index of the branch increases, while the original ResNeXt does not. This implies that the branches modify features progressively to obtain better results when more branches are used.

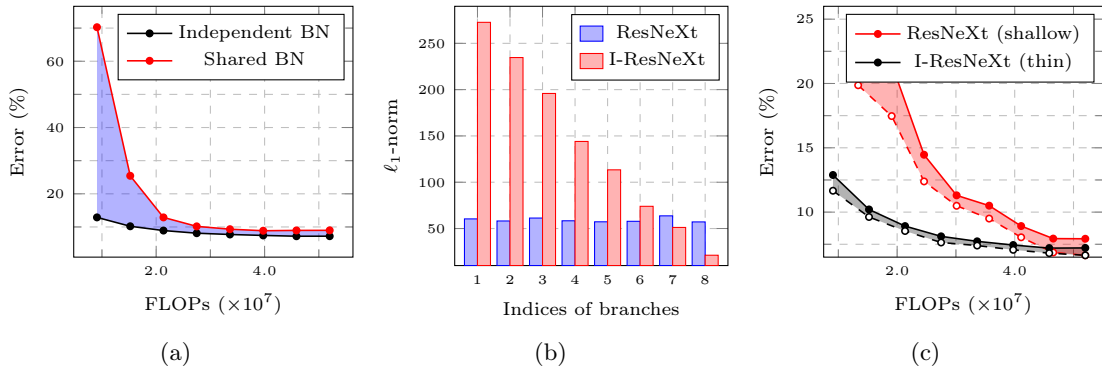


Figure 3: (a) Classification errors of thin sub-networks which are trained jointly with independent or shared BN parameters. Using independent BN layers for sub-networks can improve the overall performance. (b) ℓ_1 -norm of convolutional weights of branches. In the original ResNeXt, all branches equally contribute to construct output features. On the other hand, the contribution of branches of I-ResNeXt decreases as the index of the branch increases. (c) Shallow versus thin sub-networks for anytime prediction. The jointly trained thin sub-networks outperform shallow ones under any FLOPs. Moreover, the joint-training with thin sub-networks does not hurt their performance compared to solely trained ones.

Shallow versus thin sub-networks. To verify that using thin sub-networks is more effective for anytime prediction than shallow ones, we train shallow/thin sub-networks of ResNeXt jointly/separately and compare them. To build shallow sub-networks from a 29-layer (i.e., 9 blocks) ResNeXt, we attach $K = 8$ auxiliary classifiers to outputs of all blocks except the first one. Each classifier is of the same architecture with that used for I-ResNeXt. We use I-ResNeXt described in Section 3.1 to build $K = 8$ thin sub-networks.

We first train each sub-network separately on the CIFAR-10 dataset. The red and black dashed lines in Figure 3c are classification errors of the solely-trained shallow and thin sub-networks, respectively. As shown in the figure, one can observe that the errors of shallow networks increase rapidly as the FLOPs, i.e., the depths, decrease, e.g., the shallowest network have 19.9% error. However, the errors of thin networks drop less rapidly as all of them have 29 layers, i.e., they can capture both coarse-level and high-level features. In particular, the difference between errors of shallow and thin networks increases up to 8.2% as the required FLOPs decrease. This confirms that thin sub-networks are more effective for anytime prediction.

Next, we train all shallow (or thin) sub-networks jointly under minimizing the anytime loss (1), which is to evaluate the performance drop caused by the joint-training. The red and black solid lines in Figure 3c are the results of the joint-training with shallow and thin sub-networks, respectively. As shown in the figure, we observe that joint-training of thin sub-networks does not hurt their performance: the sub-networks lose their classification accuracy at most 1.2%. However, jointly trained shallow sub-networks lose the accuracy up to 5.1%, i.e., 4 ~ 5 times more. Consequently, jointly trained thin sub-networks, i.e., I-ResNeXt, outperform shallow ones significantly under any FLOPs. Remark that the thinnest one of I-ResNeXt has 48.4% smaller error compared to the shallowest one even though the former one has smaller FLOPs.

4.2 Results for anytime prediction

Comparisons with fixed-budget models on CIFAR. We compare our anytime prediction models, I-ResNeXt and IS-ResNeXt, with other state-of-the-art fixed-budget architectures:

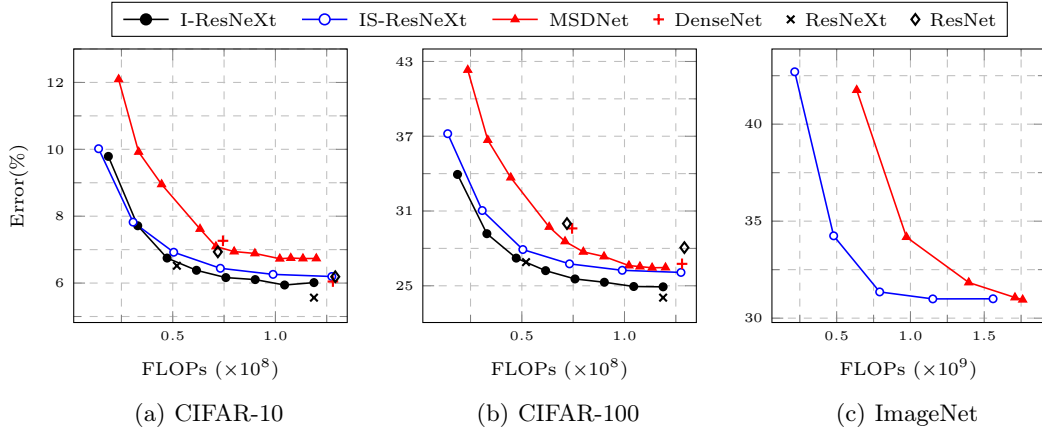


Figure 4: Top-1 classification errors of anytime prediction models (lines) and fixed-budget models (isolated points) as a function of required FLOPs on (a) CIFAR-10, (b) CIFAR-100, (c) ImageNet datasets. We obtain higher or competitive accuracy of I-ResNeXt and IS-ResNeXt compared to all other anytime and fixed-budget models, under any FLOPs or any datasets.

ResNet [13], ResNeXt [13] and DenseNet-BC [16] of various depths on the CIFAR datasets. This is to show that jointly trained sub-networks of our models can achieve better or competitive performance compared to solely trained, non-anytime prediction models, i.e., to test the optimality which is one of desired properties for anytime prediction. As shown in Figure 4a and 4b, I-ResNeXt and IS-ResNeXt have outperforming sub-networks compared to ResNet and DenseNet-BC on both CIFAR-10 and CIFAR-100 datasets. Although ResNeXt of depth 65 has the best performance at 1.2×10^8 FLOPs, I-ResNeXt has a competitive sub-network at 0.5×10^8 FLOPs.

Comparisons with MSDNet on CIFAR. Next, we indeed compare ours with the state-of-art anytime architecture, MSDNet [17] on CIFAR datasets.¹ Here, one might be interested in NestedNet models [19] to compare as they also use thin sub-networks. However, the reported performance is very poor compared to ours, e.g., a sub-network of the model has 24.5% error on CIFAR-100, while its size is 10 times larger than that of I-ResNeXt of the same error. As illustrated in Figure 4a and 4b, the full-network of I-ResNeXt has 10.7%, 5.8% relatively smaller errors on CIFAR-10 and CIFAR-100, compared to the full-network of MSDNet with respect to the same FLOPs, respectively. The sub-networks of I-ResNeXt also have up to 56.0% and 48.7% smaller FLOPs compared to those of MSDNet of the same accuracy on CIFAR-10 and CIFAR-100, respectively. Although IS-ResNeXt models are slightly worse than I-ResNeXt, they also outperforms MSDNet. For example, the thinnest sub-network of IS-ResNeXt achieves 17.2% and 12.1% relatively smaller errors, compared to the shallowest one of MSDNet on CIFAR-10 and CIFAR-100, respectively, where the former has even smaller FLOPs than the latter.

Comparison with MSDNet on ImageNet. Finally, we train IS-ResNeXt and MSDNet using the large-scale ImageNet dataset. Here, we do not try I-ResNeXt for ImageNet as it takes significantly longer.² As shown in Figure 4c, the full-network of IS-ResNeXt performs similarly to that of MSDNet, while the sub-networks of IS-ResNeXt have much higher accuracy than those of MSDNet. In particular, the gap between them increases as FLOPs decreases: sub-networks of IS-ResNeXt have up to 43.3% smaller FLOPs compared to those of MSDNet of the same accuracy. We emphasize that achieving higher performance under small FLOPs is more important for resource-limited, e.g., mobile, applications.

¹ We use a public MSDNet model released by the authors, available at <https://github.com/gaohuang/MSDNet>. For fair comparisons, we replace its classifiers by 1-layer classifiers as like ours.

² I-ResNeXt of 1.6×10^9 FLOPs requires more than 2 weeks to train ImageNet on a Titan Xp GPU.

4.3 Results for hierarchical anytime prediction

We use the CIFAR-100 and CUB datasets to evaluate the performance of IS-ResNeXt for hierarchical anytime prediction, where the coarse labels of them are obtained from their taxonomies built by WordNet [26] (see [1]). The details about the taxonomies are described in the supplementary material. All sub-networks of IS-ResNeXt are jointly trained under the hierarchical anytime loss (2). The results are illustrated in Figure 5. As expected, the finer labels are more difficult to classify and larger models can classify labels more accurately. By choosing appropriate coarse and fine labels targeted by small and large sub-networks, respectively, IS-ResNeXt maintains its performance at a certain level across all sub-networks. For example, all sub-networks can have at most 52.5% error under any budgets on the CUB dataset, while the error increases up to 68.8% without using coarse labels. At an angle, this result might not be too surprising as we improve the performance by losing the predictive information. However, the modified anytime prediction task is useful to match the original, usable accuracy in practical applications and it is remarkable that the performance of IS-ResNeXt is not degraded even under significantly more auxiliary classifiers attached.

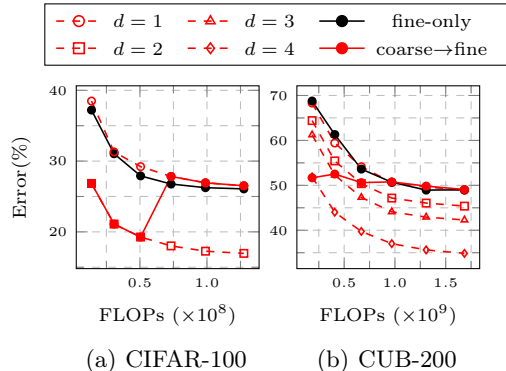


Figure 5: Top-1 classification errors of IS-ResNeXt for hierarchical anytime prediction on (a) CIFAR-100 and (b) CUB-200.

5 Conclusion

We aim for claiming that utilizing thin sub-networks of the same depth is more effective than shallow ones for anytime prediction. By focusing recent state-of-the-art multi-branch networks, we propose new models that outperforms prior ones. We also propose a new anytime prediction problem, for maintaining performance across anytime budgets via allowing rough predictions. We hope that our results would be beneficial to many related applications or problems in the future.

Acknowledgments

We would like to acknowledge Jongheon Jeong and Kimin Lee for helpful discussions, and Kibok Lee for providing the hierarchical taxonomy of the Caltech-UCSD Birds dataset. The research was funded by Naver Labs.

References

- [1] Zeynep Akata et al. “Evaluation of output embeddings for fine-grained image classification”. In: *CVPR*. 2015, pp. 2927–2936.
- [2] Tolga Bolukbasi et al. “Adaptive Neural Networks for Efficient Inference”. In: *ICML*. 2017, pp. 527–536.

- [3] Rich Caruana et al. “Intelligible models for healthcare: Predicting pneumonia risk and hospital 30-day readmission”. In: *SIGKDD*. 2015, pp. 1721–1730.
- [4] Christopher B Choy et al. “3D-R2N2: A Unified Approach for Single and Multi-view 3D Object Reconstruction”. In: *ECCV*. 2016, pp. 628–644.
- [5] Jia Deng et al. “Imagenet: A large-scale hierarchical image database”. In: *CVPR*. 2009, pp. 248–255.
- [6] Jia Deng et al. “What does classifying more than 10,000 image categories tell us?” In: *ECCV*. 2010.
- [7] Michael Figurnov et al. “Spatially Adaptive Computation Time for Residual Networks”. In: *CVPR*. 2017, pp. 1039–1048.
- [8] Xavier Gastaldi. “Shake-shake Regularization”. In: *CoRR* abs/1705.07485 (2017).
- [9] Ross Girshick. “Fast R-CNN”. In: *ICCV*. 2015, pp. 1440–1448.
- [10] Alex Grubb and Drew Bagnell. “Speedboost: Anytime Prediction with Uniform Near-optimality”. In: *AISTATS*. 2012, pp. 458–466.
- [11] Song Han, Huizi Mao, and William J Dally. “Deep compression: Compressing deep neural networks with pruning, trained quantization and huffman coding”. In: *ICLR*. 2016.
- [12] Awni Hannun et al. “Deep speech: Scaling up end-to-end speech recognition”. In: *arXiv preprint arXiv:1412.5567* (2014).
- [13] Kaiming He et al. “Deep residual learning for image recognition”. In: *CVPR*. 2016, pp. 770–778.
- [14] Kaiming He et al. “Delving deep into rectifiers: Surpassing human-level performance on imagenet classification”. In: *ICCV*. 2015, pp. 1026–1034.
- [15] Geoffrey Hinton, Oriol Vinyals, and Jeff Dean. “Distilling the knowledge in a neural network”. In: *arXiv preprint arXiv:1503.02531* (2015).
- [16] Gao Huang et al. “Densely connected convolutional networks”. In: *CVPR*. 2017.
- [17] Gao Huang et al. “Multi-scale dense convolutional networks for efficient prediction”. In: *ICLR*. 2018.
- [18] Sergey Ioffe and Christian Szegedy. “Batch Normalization: Accelerating Deep Network Training by Reducing Internal Covariate Shift”. In: *ICML*. 2015, pp. 448–456.
- [19] Eunwoo Kim, Chanho Ahn, and Songhwai Oh. “NestedNet: Learning Nested Sparse Structures in Deep Neural Networks”. In: *CVPR*. 2018.
- [20] Alex Krizhevsky and Geoffrey Hinton. *Learning multiple layers of features from tiny images*. Tech. rep. University of Toronto, 2009.
- [21] Alex Krizhevsky, Ilya Sutskever, and Geoffrey E Hinton. “Imagenet classification with deep convolutional neural networks”. In: *NIPS*. 2012, pp. 1097–1105.
- [22] Gustav Larsson, Michael Maire, and Gregory Shakhnarovich. “FractalNet: Ultra-Deep Neural Networks without Residuals”. In: *ICLR*. 2017.
- [23] Christian Ledig et al. “Photo-Realistic Single Image Super-Resolution Using a Generative Adversarial Network”. In: *CVPR*. 2017, pp. 105–114.
- [24] Hao Li et al. “Pruning filters for efficient convnets”. In: *ICLR*. 2017.
- [25] Mason McGill and Pietro Perona. “Deciding How to Decide: Dynamic Routing in Artificial Neural Networks”. In: *ICML*. 2017, pp. 2363–2372.
- [26] George A Miller. “WordNet: a lexical database for English”. In: *Communications of the ACM* 38.11 (1995), pp. 39–41.
- [27] Adriana Romero et al. “Fitnets: Hints for thin deep nets”. In: *ICLR*. 2015.
- [28] Karen Simonyan and Andrew Zisserman. “Very deep convolutional networks for large-scale image recognition”. In: *ICLR*. 2015.
- [29] Ayan Sinha et al. “SurfNet: Generating 3D Shape Surfaces Using Deep Residual Networks”. In: *CVPR*. 2017, pp. 791–800.
- [30] Christian Szegedy et al. “Going Deeper With Convolutions”. In: *CVPR*. 2015.

- [31] Surat Teerapittayanon, Bradley McDanel, and HT Kung. “Branchynet: Fast inference via early exiting from deep neural networks”. In: *ICPR*. 2016, pp. 2464–2469.
- [32] Lucas Theis et al. “Lossy Image Compression with Compressive Autoencoders”. In: *ICLR*. 2017.
- [33] Ruben Villegas et al. “Learning to Generate Long-term Future via Hierarchical Prediction”. In: *ICML*. 2017, pp. 3560–3569.
- [34] C. Wah et al. *The Caltech-UCSD Birds-200-2011 Dataset*. Tech. rep. California Institute of Technology, 2011.
- [35] Saining Xie et al. “Aggregated residual transformations for deep neural networks”. In: *CVPR*. 2017, pp. 5987–5995.
- [36] Shlomo Zilberstein. “Using Anytime Algorithms in Intelligent Systems”. In: *AI Magazine* 17.3 (1996), p. 73. ISSN: 0738-4602. DOI: 10.1609/aimag.v17i3.1232.

A Training setups

Datasets. We use CIFAR-10/100 [20], ImageNet [5] and Caltech-UCSD Birds (CUB) [34] datasets. The CIFAR datasets have 50,000 training images and 10,000 test images. Each image has 32^2 size and each pixel has RGB color. CIFAR-10/100 have 10 and 100 classes, respectively. Following [13], we use data-augmentation techniques to the training images: random horizontal flip, random-crop with 4 pixel zero-padding, normalizing pixel value by channel means and standard deviations. ImageNet has 1.2 million training images and 50,000 validation images of 1,000 classes. Similarly, CUB has 5,994 training images and 5,794 test images of 200 fine-grained bird species. For hierarchical anytime prediction, we obtain a hierarchical taxonomy of the CUB dataset from WordNet [26] by following [1]. We obtain 99 non-leaf nodes (i.e., coarse labels) from the taxonomy with maximum depth 8. By taking ancestors (i.e., coarse labels) of the leaf nodes (i.e., original fine-grained labels) up to distance 3, we build $D = 4$ different levels of labels: 200, 183, 149 and 80 labels from fine-grained to coarse-grained. Note that CIFAR-100 has its own 20 coarse-grained labels. We use the same augmentation techniques as [13] for training ImageNet and CUB images. Note that the image size after the augmentations is 224^2 .

Optimization. All models are trained by stochastic gradient descent (SGD) with Nesterov momentum of momentum 0.9 without dampening and MSRA initialization [14]. We use a weight decay of 10^{-4} and an initial learning rate of 0.1 for all experiments. The models for CIFAR and CUB are trained for 300 and 150 epochs, respectively, with a batch size of 64. The learning rate is divided by 10 after 50% and 75% epochs. For ImageNet, we use same hyperparameters as CIFAR except the learning schedule, where the total number of epochs is 90 and learning rate is divided at 30 and 60 epochs, and the batch size of 96. We randomly select 5,000, 50,000, 1,000 images of the training set for validation in CIFAR, ImageNet, and CUB datasets, respectively. Note that we use the original validation set as test set in ImageNet. All models are averaged on 5 trials.

B Details on model architectures

For I-ResNeXt and IS-ResNeXt, we denote the width of features (e.g., \mathbf{x}, \mathbf{y}) as W , the width of bottleneck features (e.g., \mathbf{a}, \mathbf{b}) as B , cardinality (or the number of branches) as C , the number of sub-networks as K and the number of blocks as L . Similarly to ResNet-based architectures, we use the same number of blocks for each scale. For down-scaling, average pooling layers of stride 2 are used with adding zero-filled features for increasing width as like the type-A shortcut connection in [13]. Note that the bottleneck width is also doubled like other ResNet models. We use 3 scales for CIFAR, and 4 scales for other datasets. It means that models for CIFAR have $32^2, 16^2, 8^2$ -sized features of $W, 2W, 4W$ channels, respectively; models for ImageNet and CUB similarly have $56^2, 28^2, 14^2, 7^2$ -sized features of $W, 2W, 4W, 8W$ channels, respectively. For all models, we use $B = 4$ as width of bottleneck in the first scale. Before the first block, we use a 3×3 convolutional layer for CIFAR images; and a 7×7 convolutional layer of stride 2 and a max pooling layer of kernel size 2 for ImageNet and CUB. We also set the cardinality by $C = 0.5W/B$ and $C = 0.75W/B$ for I-ResNeXt and IS-ResNeXt, respectively. Each classifier consists of a BN layer, a

ReLU activation, a global average pooling layer, and a fully-connected layer. Namely, the total depth of the architectures is $3L + 2$. We remind again that that all convolutional weights are shared among all sub-networks.

We use different hyperparameters for L, W, K depending on datasets and tasks. For Section 4.1 in the main paper, we use small I-ResNeXt models of $L = 9$ and $W = 64$ and build $K = 8$ thin sub-networks. In other sections, we use different hyperparameters depending on only datasets: I-ResNeXt models of $L = 21$, $W = 64$, $K = 8$ and IS-ResNeXt of $L = 15$, $W = 96$, $K = 6$ for CIFAR; IS-ResNeXt of $L = 20$, $W = 160$, $K = 5$ for ImageNet; IS-ResNeXt of $L = 16$, $W = 192$, $K = 6$ for CUB.